METTL3-mediated N6-methyladenosine modification of MMP9 mRNA promotes colorectal cancer proliferation and migration

JIE CHEN[1*], HENGLAN WU[2*], TING ZUO[3], JIANMING WU[4] and ZHIHENG CHEN[4]

[1]Department of Central Laboratory, The First Affiliated Hospital of Jiaxing University, Jiaxing, Zhejiang 314000, P.R. China;
[2]Department of Nephrology, The First Affiliated Hospital of Jiaxing University, Jiaxing, Zhejiang 314000, P.R. China;
[3]Department of Anesthesia Surgery, The First Affiliated Hospital of Jiaxing University, Jiaxing, Zhejiang 314000, P.R. China;
[4]Department of Gastrointestinal Surgery, The First Affiliated Hospital of Jiaxing University, Jiaxing, Zhejiang 314000, P.R. China

Received July 11, 2024; Accepted October 8, 2024

DOI: 10.3892/or.2024.8842

Abstract. N6-methyladenosine (m^6A) is the predominant chemical modification of eukaryotic mRNA, dynamically mediated by the RNA methyltransferase, methyltransferase-like 3 (METTL3). m^6A modification plays a critical role in cancer progression through post-transcriptional regulation in various types of cancer. However, the role of METTL3 and its associated m^6A modification in colorectal tumorigenesis remains to be fully elucidated. In the present study, it was demonstrated that METTL3 expression and the m^6A levels were both upregulated in colorectal cancer (CRC) and positively associated with clinical progression, based on the bioinformatics analysis of cancer databases. Furthermore, knockdown and overexpression of METTL3 notably affected CRC cell viability, apoptosis and migration *in vitro*. Similarly, xenograft animal models confirmed that METTL3 promoted CRC tumorigenicity *in vivo*. Mechanistically, it was revealed that the m^6A modification of matrix metallopeptidase 9 (MMP9) mRNA mediated by METTL3 promoted its expression in CRC by decreasing its degradation. Collectively, the findings of the present study suggested that the METTL3/MMP9 axis could serve as a novel promising therapeutic candidate for CRC.

Introduction

Colorectal cancer (CRC) ranks as the third most frequently diagnosed cancer in both women and men and is a major cause of cancer-related mortality globally (1). The survival outcomes of CRC remain poor, partially owing to the presence of distant metastases (2). Specifically, the 5-year survival rate decreases to 8% for patients with CRC and advanced metastasis (3). Despite improvements in the diagnosis and treatment strategies for CRC at an unparalleled pace in recent years, the prognosis of advanced CRC remains poor, which is largely due to the mechanisms that underlie the induction of CRC progression remaining unexplained (4). Due to the scarcity of powerful therapeutic strategies in CRC, new pathways and targets against this carcinoma need to be unearthed. A growing body of evidence has shown that genetic and epigenetic alterations contribute to the pathogenesis of CRC (5-7). Therefore, interrogating genetic and epigenetic factors that drive tumor progression and constructing more accurate models for prognostic prediction in CRC are urgently needed.

N6-methyladenosine (m^6A) modification is garnering increasing interest as a prevalent epigenetic modification of eukaryotic mRNA, affecting multiple steps of RNA metabolism including RNA splicing, maturation, nuclear export and translation (8-10). The m^6A RNA modification is a dynamic and reversible process coordinated by a methyltransferase complex (m^6A 'writer'), demethylases (m^6A 'erasers') and m^6A-binding proteins (m^6A 'readers') (11). The m^6A methylase complex is comprised of at least five writer proteins [methyltransferase like-3 (METTL3), METTL14, WT1 associated protein (WTAP), vir-like m6A methyltransferase associated and RNA binding motif protein 15/15B), among which METTL3 protein serves a central role (12-15). The erasers, human Alk B homolog-5 (ALKBH5) and fat mass and obesity-associated gene (FTO), have m^6A demethylation activity to specifically remove the m^6A modification (16,17). METTL3, acting as an oncogene, maintains SRY-box transcription factor 2 (SOX2) expression by preventing SOX2 mRNA degradation via m^6A/insulin like growth factor 2 mRNA binding protein 2 (IGF2BP2) axis regulation, thus contributing to the progression of CRC (18). Additionally, METTL3 facilitates the progression of CRC by upregulating Janus kinase 1 and STAT3 expression through both m^6A-dependent and -independent mechanisms, consequently activating the phosphorylated-STAT3 signaling pathway (19). Moreover, METTL3 is upregulated in human CRC and promotes CRC progression by elevating MYC expression and epigenetically attenuating the expression of

Correspondence to: Professor Zhiheng Chen, Department of Gastrointestinal Surgery, The First Affiliated Hospital of Jiaxing University, 1882 Zhonghuan South Road, Nanhu, Jiaxing, Zhejiang 314000, P.R. China
E-mail: chenzh1979@163.com

*Contributed equally

Key words: N6-methyladenosine, methyltransferase-like 3, colorectal cancer, matrix metallopeptidase-9, proliferation, migration

the yippee-like 5 tumor suppressor, as well as stabilizing cyclin-E1 mRNA via m^6A mRNA modification of the effectors (20-22). These studies unrevealed that m^6A modification and METTL3 regulation play pivotal roles in tumorigenesis, tumor development and metastasis, and the dysregulation of m^6A is closely associated with the development and pathogenesis of CRC. Nevertheless, m^6A modification play a central role in various cancer types and the definite role of m^6A in CRC remains obscure, and the dysregulation of METTL3-mediated m^6A modification in the progression of CRC requires further investigation.

Matrix metallopeptidase (MMP)-9 and MMP2 participate in angiogenesis by remodeling the extracellular matrix (ECM), activating and deactivating ECM components by proteolysis cleavage, and are thus involved in cancer cell proliferation and differentiation (23). MMP9 inhibition significantly decreased primary tumor growth and the incidence of metastasis in a surgical CRC orthotopic xenograft model (24). A number of findings have revealed that MMP9 plays a crucial role in tumor progression, with the MMP9 expression level correlating with the grade and stage of carcinoma (25-27). However, the relationship between m^6A-related factors and MMP9 in CRC progression outcomes are not well defined.

The present study aimed to explore the role of m6A modification and its key regulator, METTL3, in the progression of CRC. The primary objectives were to assess the expression levels of m6A and m6A-related regulators in CRC tissues and to investigate the functional impact of METTL3 on CRC cell behavior. To achieve these aims, the study employed a multi-faceted approach that included both *in vitro* and *in vivo* experiments. The *in vitro* component involved the use of cell cultures to manipulate the expression levels of METTL3 and to observe the subsequent effects on CRC cell proliferation, migration and apoptosis. By combining these methods, the study aimed to provide a comprehensive understanding of the METTL3/MMP9 axis in CRC and to establish a foundation for the development of novel therapeutic strategies targeting this axis. The results of these experiments are expected to contribute significantly to the field by offering insights into the molecular mechanisms underlying CRC and potentially leading to more effective treatments.

Materials and methods

Cell culture. In total, three CRC cell lines (LS174T, HCT116 and SW480) and two normal human colon mucosal epithelial cell lines (NCM-460 and HIEC-6) were utilized in the present study, all acquired from The Cell Bank of Type Culture Collection of The Chinese Scientific Academy. The HCT116, SW480, NCM-460 and HIEC-6 cell lines were regularly maintained in RPMI-1640 medium with 10% fetal bovine serum (FBS) and 1% penicillin-streptomycin (all from Gibco; Thermo Fisher Scientific, Inc.) in a humidified incubator set at 37˚C and 5% CO_2. Conversely, the LS174T cells were cultured using Dulbecco's Modified Eagle's Medium (Gibco; Thermo Fisher Scientific, Inc.) supplemented with 10% FBS and 1% penicillin-streptomycin.

Establishment of stable knockdown and overexpression cell lines. To perform RNA interference, HCT116 and SW480 cells were seeded in 60 mm tissue culture plates for 24 h prior to transfection. METTL3 short hairpin (sh)RNA cloned into the pLKO.1 lentiviral vector (Addgene, Inc.) was obtained. Subsequently, the vector (pLKO.1-METTL3) was co-transfected into CRC cells with the psPAX2 and pmD2G (Addgene, Inc.) packing plasmids at a 4:3:1 ratio, using the PolyJet reagent (SignaGen Laboratories) in serum-free media. After 48 h transfection at 37˚C, the cell culture supernatant was harvested and filtered through a 0.22 μm membrane. Following concentration using a 100 kD Millipore filter, the viral solution was added to the cancer cell culture medium at a multiplicity of infection of 3, allowing for a 24-h infection period. Successfully transfected cells expressing shRNAs were selected using 5 μg/ml puromycin (Sigma-Aldrich; Merck KGaA) and maintained in RPMI-1640/10% FBS supplemented with 1 μg/ml puromycin at 37˚C and 5% CO_2. The sequences of the shRNAs were as follows: sh-METTL3, 5'-GCACTTGGATCTACGGAA TCC-3'; and sh negative control (NC), 5'-GTCCATCGAACT CAGTAGCT-3'.

To achieve METTL3 overexpression, HCT116 cells were stably transfected with the pcDNA3/Flag-METTL3 plasmid (cat. no. 53739; Addgene, Inc.). HCT116 and SW480 cells were stably transfected with the pcDNA3-MMP9 plasmid (Suzhou Hongxun Biotechnologies Co., Ltd.). The transfection procedure was conducted utilizing Lipofectamine 3000 (Invitrogen; Thermo Fisher Scientific, Inc.) following the manufacturer's instructions. Briefly, the cells were grown in 6-well plates until they reached 90% confluency. Then, the cells were transfected with plasmid DNA (5.0 mg per well), utilizing Lipofectamine 3000 (10 μl) to facilitate transfection at 37˚C. After 48 h, the cells were subjected to trypsinization and subsequently transferred to 10-cm culture dishes in medium supplemented with 300 mg/ml G418 (Gibco; Thermo Fisher Scientific, Inc.) and maintained with 50 mg/ml G418. Clonal expansion was achieved through the isolation of single-cell clones.

mRNA m^6A quantification. Total RNA was isolated using the TRIzol reagent (Ambion; Thermo Fisher Scientific, Inc.). Subsequently, the polyadenylated RNA was extracted from the total RNA using the Dynabeads™ mRNA Purification Kit (Invitrogen; Thermo Fisher Scientific, Inc.), with any contaminating rRNA removed by the RiboMinus transcriptome isolation kit (Invitrogen; Thermo Fisher Scientific, Inc.). The relative levels of m^6A in the mRNA were assessed utilizing an m^6A RNA Methylation Quantification Kit (Colorimetric; cat. no. P-9005; EpigenTek Group, Inc.), according to the manufacturer's instructions. Briefly, capture and detection antibodies were employed to measure the m^6A levels, which were determined at measuring the absorbance at 450 nm. Each reaction was replicated three times to quantify the relative absorbance.

RNA extraction, reverse transcription (RT) and quantitative PCR (qPCR). Total cellular RNA was isolated using the RNA isolation kit (Shanghai Yeasen Biotechnology Co., Ltd.) and subsequently reverse transcribed into cDNA with the PrimeScript™ RT Reagent Kit, which included a gDNA Eraser (Takara Bio, Inc.). qPCR was conducted using the TB Green® Premix Ex Taq™ (Takara Bio, Inc.). The qPCR thermocycling conditions were as follows: 40 cycles at 37˚C for

15 min, 60˚C for 5 sec and 72˚C for 30 sec. The relative mRNA expression levels were calculated using the $2^{-\Delta\Delta Cq}$ method (28). All procedures followed the manufacturer's instructions and were repeated three times. The primer (Sangon Biotech Co., Ltd.) sequences were as follows: METTL3 forward, 5'-CTA TCTGGCACTCGCAAGA-3' and reverse, 5'-GCTTGAACC GTGCAACCACATC-3'; MMP9 forward, 5'-CCAATCACC ACCATCCGTTG-3' and reverse, 5'-CCTCGGGCAAAT GTCTTACC-3'; GAPDH forward, 5'-GTCTCCTCTGACTTC AACAGCG-3' and reverse, 5'-ACCACCCTGTTGCTGTAG CCAA-3'; and 18S forward, 5'-GGAGTATGGTTGCAAAGC TGA-3' and reverse, 5'-ATCTGTCAATCCTGTCCGTGT-3'.

m^6A-modified RNA immunoprecipitation. Stable knockdown METTL3 cell RNA was extracted, and polyadenylated RNA was enriched using an mRNA purification kit (Thermo Fisher Scientific, Inc.). This enriched RNA was then treated with DNase I (Thermo Fisher Scientific, Inc.). Following this, 100 μg global RNA was incubated with m^6A or IgG antibodies for immunoprecipitation using the Magna methylated RNA immunoprecipitation (MeRIP) m^6A kit (cat. no. 17-10499; MilliporeSigma) according to the manufacturer's instructions. For m6A RIP qPCR, the total RNAs were fragmented into 300-nucleotide fragments after incubation in fragmentation buffer at 94˚C for 30 sec and immunoprecipitated using anti-m6A antibody according to the manufacturer's instructions. In total, one-tenth of the fragmented RNAs were saved as input control, and the enrichment of m6A was quantified using RT-qPCR.

RNA half-life assay and qPCR. To assess the degradation rate of MMP9 mRNA, cells were treated with Actinomycin-D (Act-D; Sigma-Aldrich; Merck KGaA) at a final concentration of 3 μg/ml at 37˚C to inhibit new RNA synthesis. At specified intervals, cell samples were collected and analyzed using qPCR (as aforementioned). The MMP9 expression levels were standardized against 18S RNA.

Protein stability assay. To measure protein stability, shNC and shMETTL3 transfected cells were seeded into 6-well plates and treated with cycloheximide (Cayman Chemical Company; to inhibit RNA translation) at 37˚C at final concentration of 20 μg/ml for the indicated times. Cells were collected and lysed in RIPA lysis buffer (Cell Signaling Technology, Inc.). The expression of proteins was measured through western blot analysis.

Cell viability assay. In total, 100 μl of culture medium containing $3x10^4$ cells were seeded into 96-well plates and cultured for 24 h. Subsequently, 10 μl Cell Counting Kit-8 (CCK-8) reagent (Dojindo Laboratories, Inc.) was added to each well. Following an additional 2-h incubation in a humidified environment at 37˚C with 5% CO_2, the absorbance of the cells at 450 nm was measured using a spectrophotometer. Each assay was performed in triplicate.

Cell migration and invasion assays. To assess the migration capability, $1x10^6$ cells per well were cultured in 6-well plates until a 80-90% confluency was reached. A sterile 200 μl pipette tip was employed to create straight uniform scratches. Cells were serum-starved prior to and during the assay. Images were obtained by light microscopy (Nikon C1 Eclipse; Nikon Corporation) and captured at both 0 and 48 h, with each experimental condition tested in triplicate. Image analysis was performed using ImageJ (version1.42q; National Institutes of Health). The relative scratch width was expressed as: (original scratch width-new scratch width)/original scratch width x100%.

For evaluating the invasion capability, Transwell chambers pre-coated with Matrigel (BD Biosciences) at 37˚C for 4 h were utilized. The upper chamber contained the specific cells ($1x10^4$ cells) in serum-free medium, while the lower chamber contained complete medium supplemented with 10% FBS. Cells that invaded the surface of the lower chamber after 24 h were then fixed with 4% paraformaldehyde for 15 min and stained with 0.1% crystal violet (Beijing Solarbio Science & Technology Co., Ltd.) for 3 min at room temperature. After air drying, the invaded cells were imaged using a light microscope (Nikon C1 Eclipse; Nikon Corporation) and quantified by counting cells in five randomly selected fields. Image analysis was performed using ImageJ (version1.42q; National Institutes of Health).

Apoptosis assays. To evaluate apoptosis, flow cytometry was employed utilizing a FITC-Annexin V/PI detection kit (Wanleibio, Co., Ltd.). Each well was seeded with $1x10^6$ cells in 6-well plates, followed by harvesting after 48 h of incubation at 37˚C. The cells were then stained with FITC-Annexin V and PI for 15 min at room temperature, in the dark. Apoptotic cell percentages were subsequently determined through FACS flow cytometry (FACS Canton II; BD Biosciences) and the data were analyzed using FlowJo 8.6.3 (Tree Star, Inc.).

Protein isolation and western blotting. Cellular proteins were extracted utilizing RIPA buffer (cat. No. 9806; Cell Signaling Technology, Inc.) supplemented with a protease and phosphatase inhibitor cocktail (Sigma-Aldrich; Merck KGaA). Protein concentrations were quantified using a BCA Protein Assay kit (Beyotime Institute of Biotechnology). The proteins (20 μg per lane) were resolved on 10% SDS-PAGE gels and subsequently transferred PVDF membranes. To block non-specific binding, the membranes were incubated with 5% non-fat milk in TBST (0.1% Tween-20) for 2 h at room temperature. Following this, the membranes were incubated overnight at 4˚C with primary antibodies against METTL3 (1:2,000; cat. no. 86132S; Cell Signaling Technology, Inc.), MMP9 (1:1,000; cat. no. ab76003; Abcam) and GAPDH (1:5,000; cat. no. 5174S; Cell Signaling Technology, Inc.). After three washes with PBST (0.1% Tween 20), the membranes were incubated for 1 h at room temperature with a horseradish peroxidase (HRP)-conjugated secondary antibody (1:1,000; cat. no. BA1055; Boster Biological Technology). The signal was detected using ECL western blotting detection reagents (Tanon Science and Technology Co., Ltd.). Quantification of protein expression levels was performed using ImageJ software (version 1.50; National Institutes of Health).

Xenograft animal models. HCT116, METTL3 knockdown HCT116 and METTL3 overexpressing HCT116 cells ($5x10^6$ cells; n=5 mice per group) were suspended in 100 μl PBS and

Matrigel (Shanghai Yeasen Biotechnology Co., Ltd.) at a 1:1 ratio. This cell mixture was then subcutaneously injected into the flanks of 4-week-old nude mice (weighing 14-16 g). All 15 mice were placed in SPF housing conditions with a 12:12-h light/dark cycle and at a constant temperature (22±2˚C). Furthermore, the mice were given unrestricted access to standard chow and water. Throughout the experimental period, mice were monitored three times a week for tumor development. The tumors were measured using calipers, with a humane endpoint set at a tumor diameter of >2,000 mm. The tumor volume was calculated using the following formula: Volume=W^2 x L/2, where W represents the short diameter and L represents the long diameter. The weights of the mice were rigorously monitored to ensure that any decrease did not exceed 20%, thereby mitigating potential suffering. No animals died before meeting the criteria for humane endpoint euthanasia. At the end of the experiment (day 24), the mice were anesthetized through intraperitoneal administration of sodium pentobarbital (50 mg/kg) and subsequently sacrificed by cervical dislocation. Following euthanasia, the xenograft tumors were carefully excised from the sacrificed mice and weighed immediately. The experiments adhered to institutional guidelines and ethical standards regarding euthanasia and death verification. Some tumor specimens were used for RNA extraction with TRIzol, followed by qPCR to assess the METTL3 and MMP9 mRNA expression levels (as aforementioned). The remaining samples were fixed with 10% (v/v) neutral-buffered formalin for 24 h at room temperature, then transferred to 70% ethanol until they were embedded in paraffin and sectioned at a 3 μm thickness. For hematoxylin-eosin staining, the sections were treated with hematoxylin for 2 min and eosin for 1 min.

Immunohistochemistry (IHC). Antigen retrieval was performed using boiling sodium citrate buffer (0.1 M, pH 4). After deparaffinization and hydration of the paraffin-embedded tissue sections, endogenous peroxidase activity was blocked with Peroxidase 1 blocking reagent (Biocare Medical, LLC) for 10 min followed by blocking with Background Sniper serum-free blocking reagent (Biocare Medical, LCC) for 15 min at room temperature. Tissue sections were incubated overnight at 4˚C with primary antibodies targeting METTL3 (1:50; cat. no. 86132S; Cell Signaling Technology, Inc.), MMP9 (1:1,000; cat. no. ab76003; Abcam) and Ki67 (1:100; cat. no. ab16667; Abcam). Post incubation, sections were washed with PBST (0.05% Tween-20) and then treated with a HRP-conjugated rabbit secondary antibody (1:5,000; cat. no. BM3894; Wuhan Boster Biological Technology, Ltd.) at room temperature for 1 h. The sections were subsequently developed using 0.05% 3-diaminobidine tetrahydrochloride for 10 sec at room temperature, followed counterstaining with 10% Mayer's hemoxylin for 4 min at room temperature. The IHC results were analyzed by two experienced pathologists. For imaging, five random fields at x200 magnification under a light microscope (Leica DMI4000B; Leica Microbiosystems GmbH) were selected.

Bioinformatics analysis. The Gene Expression Profiling Interactive Analysis database (gepia.cancer-pku.cn/) served as the tool to assess the mRNA expression levels of METTL3, METTL14, WTAP, ALKBH5 and FTO in both CRC and normal tissues. For Kaplan-Meier analysis, the log-rank test was employed. To determine the overall survival of patients with CRC and varying levels of METTL3 expression, Kaplan-Meier survival analyses were performed using the Kaplan Meier plotter online tool (http://kmplot.com/analysis/) with default parameters. The median value was set as the cut-off.

Statistical analysis. Each experiment was conducted a minimum of three times, with representative outcomes illustrated. Data are presented as the mean ± SD. One-way analysis of variance with Tukey's multiple comparisons was used to identify significant differences among three or more groups, while two groups were compared using the unpaired Student's t-test. Data analysis was performed using GraphPad Prism 8 software (Dotmatics). $P<0.05$ was considered to indicate a statistically significant difference.

Results

Upregulation of METTL3 and m^6A is associated with clinicopathological features in CRC. To investigate the role of m^6A modification in CRC *in vitro*, the m^6A levels in three CRC cell lines (LS174T, HCT116 and SW480) and two normal human colon mucosal epithelial cell lines (HIEC-6 and NCM-460) were quantified using the colorimetric m^6A quantification assay. The results demonstrated that the global mRNA m^6A levels were elevated in the CRC cell lines compared with the normal cell lines (Fig. 1A). To assess the expression profiles of m^6A writers and erasers in CRC, The Cancer Genome Atlas database was analyzed, and it was found that METTL3 was upregulated in CRC clinical tissues (Fig. 1B). The RT-qPCR results further indicated a significant increase in METTL3 expression in CRC cell lines, particularly in HCT116 and SW480 cells, compared with the normal epithelial cell lines (Fig. 1C). These findings suggest that METTL3, an RNA methyltransferase, may play a crucial role in CRC progression. Moreover, METTL3 expression was higher in advanced clinical stages than in the early stages, showing a significant positive association (Fig. 1D). Kaplan-Meier survival curves indicated that higher METTL3 expression was significantly associated with a lower survival rate among patients with CRC (Fig. 1E). Thus, these results indicate that METTL3 is highly expressed in CRC and is associated with poor prognosis.

Knockdown of METTL3 blocks metastatic characteristics in CRC. To explore the role of METTL3 in the progression of CRC as suggested by the clinical data, the proliferation and invasion capabilities of CRC cells were examined. For this purpose, two stable CRC cell lines with METTL3 knockdown were established using different shRNAs delivered via lentivirus. Validation of METTL3 knockdown at the mRNA level showed a reduction of 25% in HCT116 cells and 45% in SW480 cells (Fig. 2A). Correspondingly, the METTL3 protein levels were significantly lower in the knockdown cells compared with the controls. Densitometric analysis confirmed a 20% decrease in METTL3 protein in HCT116 cells and a 43% decrease in SW480 cells (Fig. 2B). RT-qPCR and western blotting therefore demonstrated the notable METTL3 knockdown efficiency of the lentivirus used. The

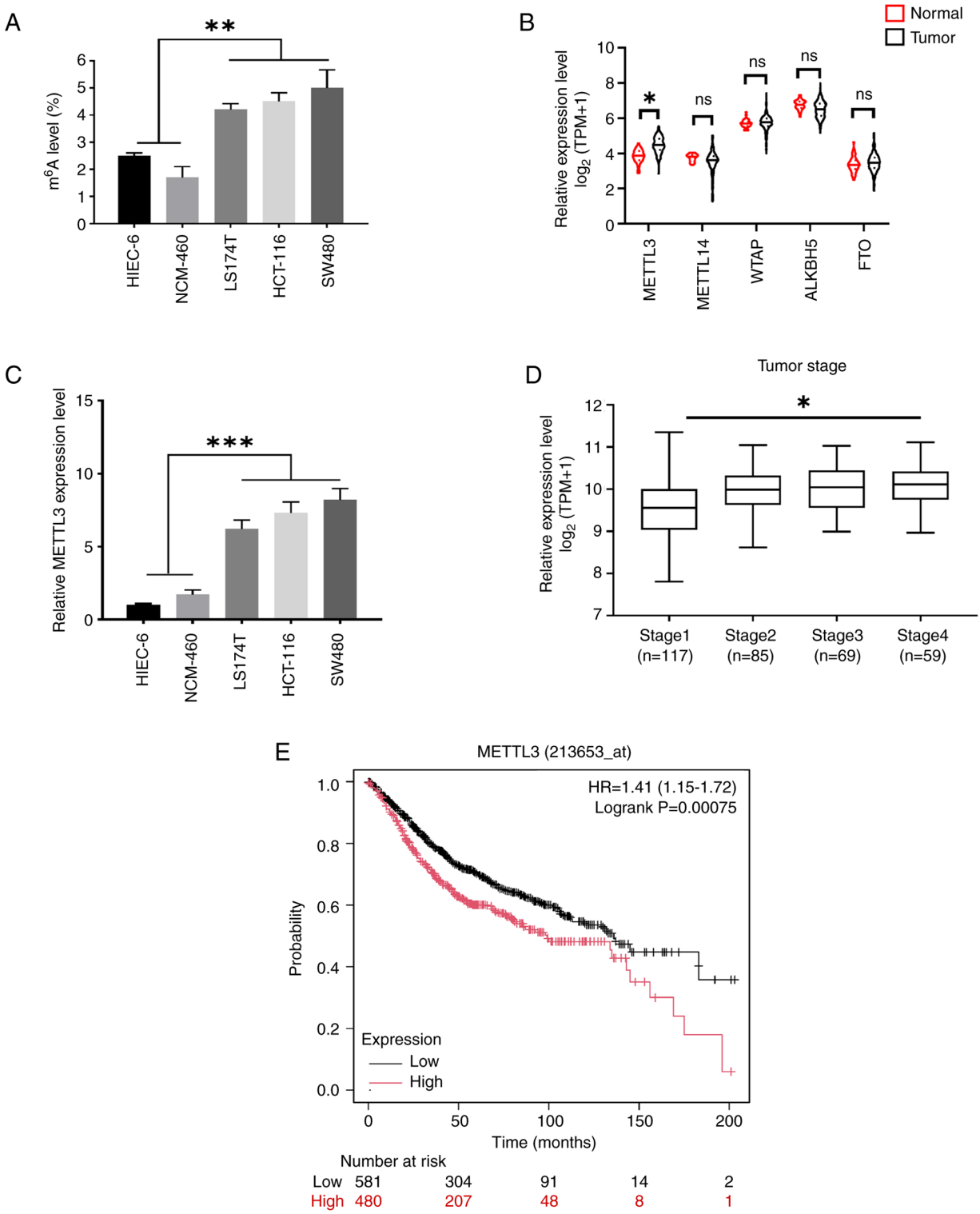

Figure 1. Upregulation of m^{6}A and METTL3 in colorectal cancer. (A) Total mRNA m^{6}A levels in colorectal cancer cell lines compared with normal human colonic epithelial cell lines was detected by m^{6}A-immunoprecipitated quantitative PCR. (B) Bioinformatics analysis of METTL3 in tumor vs. normal colorectal tissues in the Gene Expression Profiling Interactive Analysis database. (C) The METTL3 expression levels in CRC cell lines compared with normal human colonic epithelial cell lines. (D) The METTL3 expression levels in tumors of different clinical stages of CRC was depicted by box plot. (E) Kaplan-Meier overall survival analysis of patients with CRC. Error bars, SD. *P<0.05, **P<0.01, ***P<0.001. METTL3, methyltransferase-like 3; CRC, colorectal cancer; m^{6}A, N6-methyladenosine; TPM, transcripts per million; ns, not significant; WTAP, WT1 associated protein; ALKBH5, Alk B homolog-5; FTO, fat mass and obesity-associated gene; HR, hazard ratio.

stable with/without METTL3 knockdown (shMETTL3 and shNC) HCT116 and SW480 cells were employed to investigate the influence of METTL3 on the proliferation and migration capacity. The CCK-8 assay results demonstrated a significant downregulation of the viability of the shMETTL3 HCT116 and SW480 cells (Fig. 2C). Additionally, the Transwell and scratch assays demonstrated that shMETTL3 cells exhibited reduced invasion (Fig. 2D) and migration (Fig. 2E) capacities

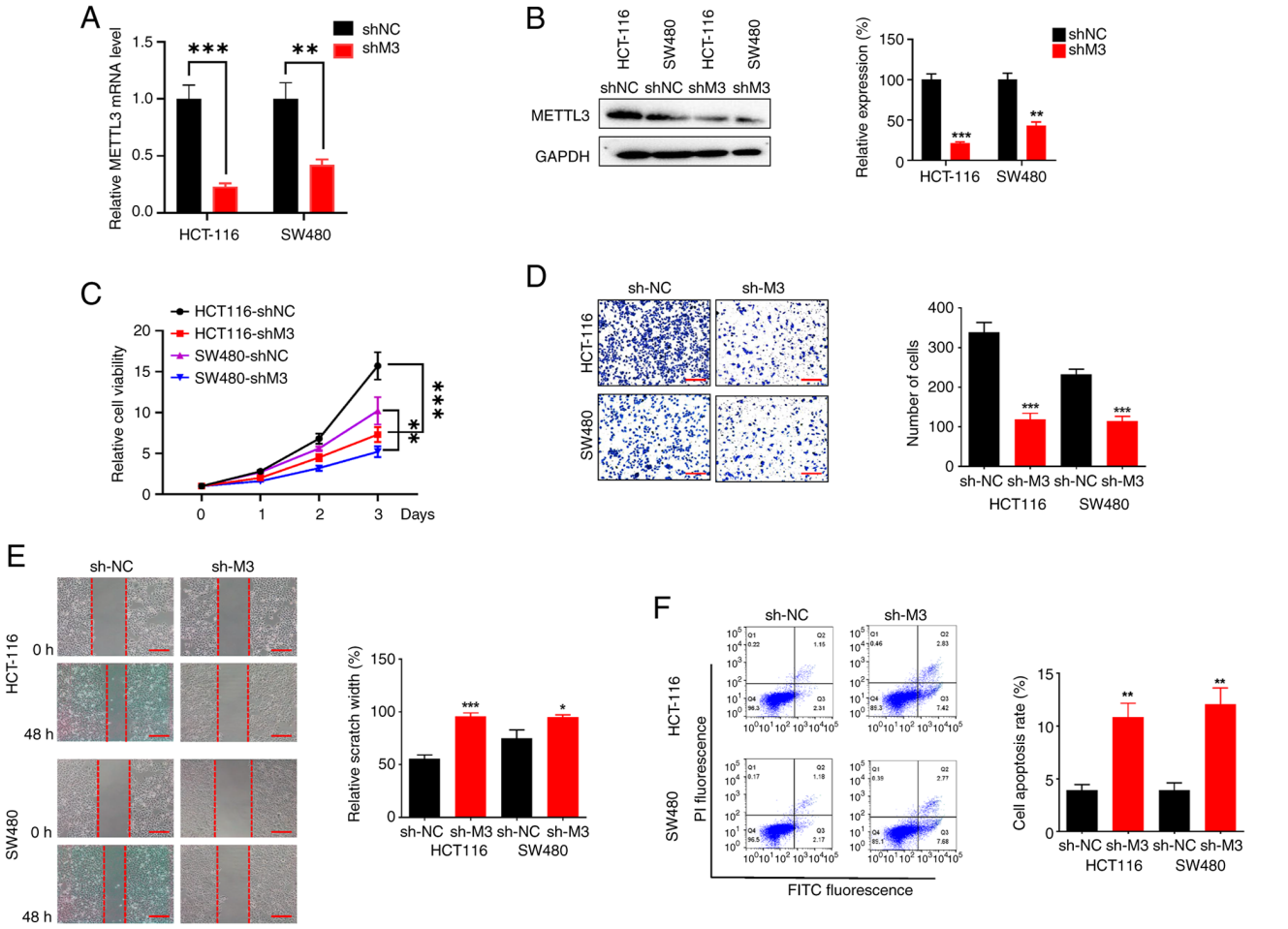

Figure 2. Promoting role of METTL3 in colorectal cancer cells. (A) Relative METTL3 mRNA levels in stable METTL3 knockdown HCT116 and SW480 cell lines was detected by quantitative PCR. (B) Relative METTL3 protein levels in the two stable METTL3 knockdown CRC cell lines. (C) The effect of METTL3 knockdown on CRC cell proliferation was investigated using Cell Counting Kit-8 assays. (D) The invasion ability of HCT116 and SW480 cells was examined by Transwell assay following METTL3 knockdown. Scale bars, 100 μm. (E) The migration ability of HCT116 and SW480 cells was examined by wound healing assay following METTL3 knockdown. Scale bars, 100 μm. (F) The influence of METTL3 knockdown on cell apoptosis was detected by flow cytometry. Error bars, SD. *P<0.05, **P<0.01, ***P<0.001. METTL3/M3, methyltransferase-like 3; CRC, colorectal cancer; sh, short hairpin (RNA); NC, negative control.

compared with shNC cells. Flow cytometry further showed that METTL3 knockdown increased apoptosis in CRC cell lines (Fig. 2F). Overall, these results suggest that knocking down METTL3 decreases cell viability and migration while promoting apoptosis in CRC cell lines.

MMP9 is regulated by METTL3-mediated m^{6}A modification. MMP9 plays a promotive role in various cancer types; DNA methylation of the MMP9 gene has been shown to result in the upregulation of MMP9 protein expression, thereby facilitating cancer progression and metastasis (29). We hypothesized that METTL3 may regulate the expression of MMP9 in an m^{6}A-dependent manner, further participating in CRC tumorigenesis via post-transcriptional regulation. The level of MMP9 m^{6}A methylation in shMETTL3 and shNC cells were first examined by employing the MeRIP assay. The results of the m^{6}A quantification assays implied that the MMP9 mRNA m^{6}A modification levels were higher in HCT116 shNC cells (Fig. 3A) and SW480 shNC cells (Fig. 3B) compared with shMETTL3 cells. Moreover, western blotting showed that the expression of MMP9 protein was downregulated in shMETTL3 cells compared with shNC cells in the two CRC cell lines (Fig. 3C). In METTL3-knockdown HCT116 and SW480 cells, the expression level of MMP9 mRNA was also significantly reduced (Fig. 3D). Next, the mechanisms behind METTL3-mediated regulation of MMP9 in CRC cells were explored by determining the protein and mRNA stability. Results from the western blotting analysis showed that the half-lives of MMP9 protein in shMETTL3 cells was comparable to that of shNC cells in both the HCT116 (Fig. 3E) and SW480 (Fig. 3F) cell lines, suggesting that decreased METTL3 expression was not related to protein stability. Given the reduced mRNA levels of MMP9 in METTL3-knockdown cells, we hypothesized that m^{6}A modification might influence MMP9 mRNA stability. After treating cells with Act-D to assess mRNA abundance, the stability of mature mRNA in shMETTL3 cells was significantly lower compared with their shNC counterparts (Fig. 3G). This suggested that the mRNA stability of MMP9 was decreased in METTL3-knockdown CRC cells.

To further characterize the role of MMP9, METTL3 and MMP9 protein interactions were studied using a

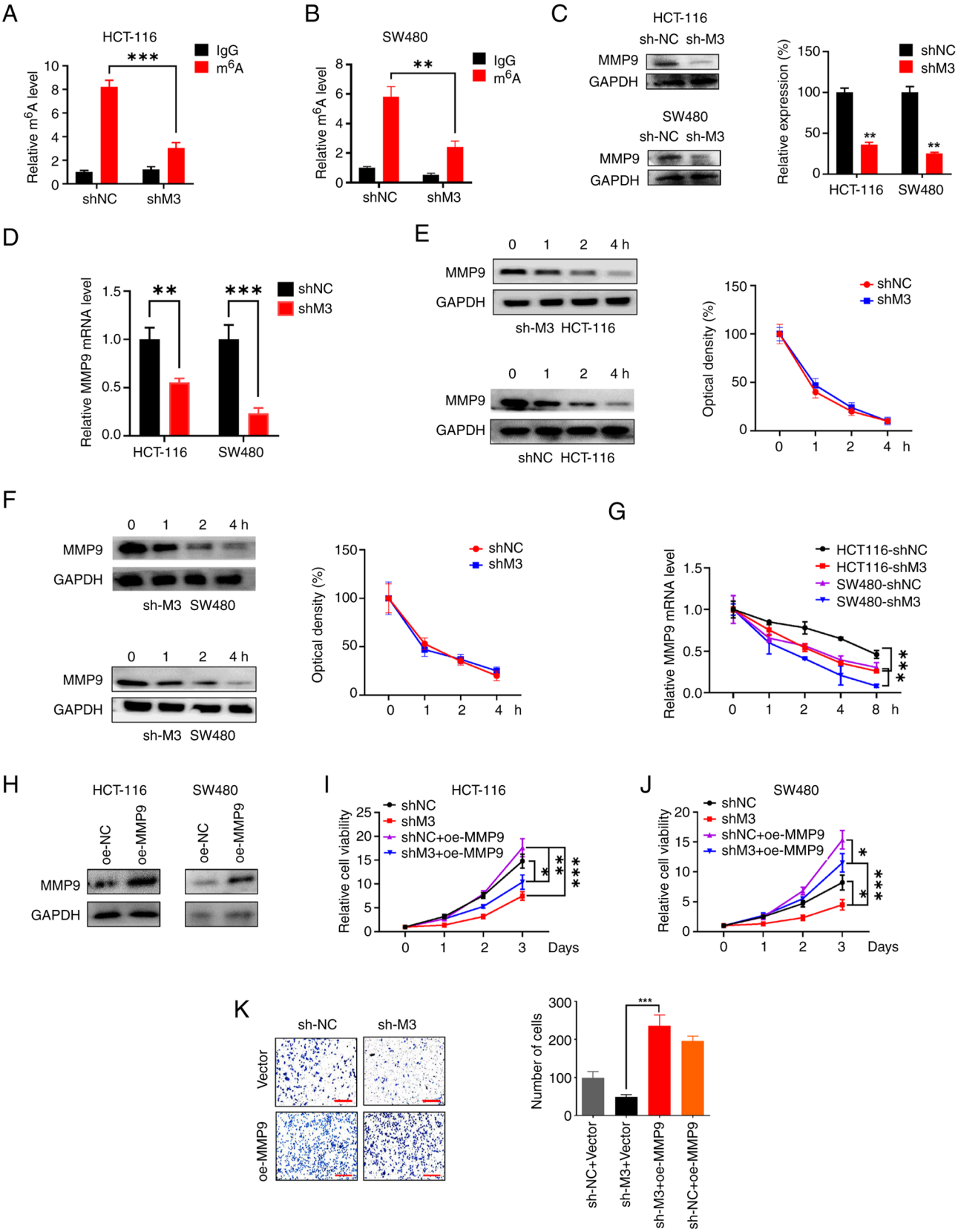

Figure 3. METTL3 stabilizes MMP9 mRNA in a m^{6}A-dependent manner. MMP9 mRNA m^{6}A levels of stable METTL3 knockdown (A) HCT116 and (B) SW480 cell lines was detected by m^{6}A-immunoprecipitated qPCR. The (C) protein and (D) mRNA levels of MMP9 in METTL3-knockdown HCT116 and SW480 cells. MMP9 protein expression levels in shNC and shMETTL3 (E) HCT116 and (F) SW480 cell lines treated with cycloheximide (20 μg/ml) for the indicated time points were detected by western blotting. (G) MMP9 mRNA expression levels in shNC and shMETTL3 cells treated with Actinomycin (5 μg/ml) for the indicated time points were detected by qPCR. (H) Western blot analysis of MMP9 expression in oe-MMP9 cells was performed. The viability of (I) HCT116 and (J) SW480 cells with or without METTL3 knockdown after transfection with oe-MMP9 were determined by Cell Counting Kit-8 assay. (K) The invasion ability of HCT116 and SW480 cells with or without METTL3 knockdown after transfection with oe-MMP9 was determined by Transwell assay. Scale bars, 100 μm. Error bars, SD. *P<0.05, **P<0.01, ***P<0.001. m^{6}A, N6-methyladenosine; METTL3/M3, methyltransferase-like 3; MMP9, matrix metallopeptidase 9; CRC, colorectal cancer; qPCR, quantitative PCR; sh, short hairpin (RNA); NC, negative control; oe, overexpression.

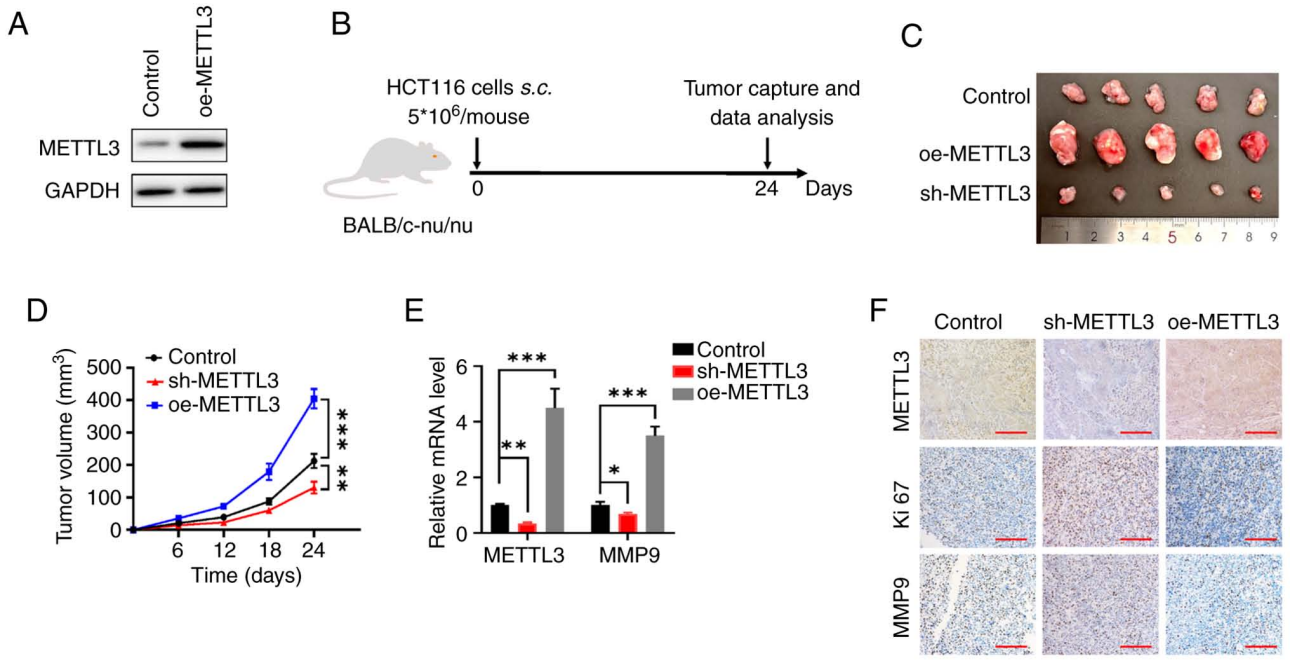

Figure 4. METTL3 promotes colorectal cancer cell progression *in vivo*. (A) Western blot analysis of METTL3 was performed on HCT116 cells transfected with oe-METTL3. (B) Flow chart of the *in vivo* experimental design. (C) Xenograft assay was performed using HCT116 cells transfected with sh-METTL3, oe-METTL or empty vector (pcDNA3; control). (D) Quantitative analysis of the xenograft tumor volume. (E) The METTL3 and MMP9 mRNA levels in tumor tissues expressing sh-METTL3 or oe-METTL3 or the control HCT116 cells. (F) Expression of METTL3, Ki67 and MMP9 was detected by immunohistochemistry of paraffin-embedded tissues. Scale bars, 100 μm. Error bars, SD. *P<0.05, **P<0.01, ***P<0.001. METTL3, methyltransferase-like 3; MMP9, matrix metallopeptidase 9; sh, short hairpin (RNA); NC, negative control; oe, overexpression; s.c., subcutaneous.

gain-and-loss functional experiment system. For this purpose, stable MMP9-overexpression HCT116 and SW480 cell lines were constructed and western blotting was utilized to verify MMP9 expression (Fig. 3H). The CCK-8 results showed that downregulation of METTL3 attenuated the cell viability; furthermore, overexpression of MMP9 fostered the sh-METTL3-induced downregulation of cell viability in HCT116 cells (Fig. 3I). Similar results were observed in SW480 cells, in which overexpression of MMP9 restored the shMETTL3-induced downregulation of cell viability (Fig. 3J). Additionally, the Transwell assay result showed that the MMP9 overexpression could prevent the inhibition of cell invasion caused by METTL3-knockdown (Fig. 3K). Therefore, the results indicated that METTL3 facilitates CRC tumorigenesis by enhancing the expression of MMP9 through m^{6}A modification and downregulating the decay rate of MMP9 mRNA.

METTL3 facilitates CRC tumorigenesis by enhancing the expression of MMP9 in vivo. Stable METTL3-overexpression HCT116 cells were constructed and western blotting was utilized to verify METTL3 expression (Fig. 4A). To investigate the role of METTL3 *in vivo*, a subcutaneous xenotransplantation model was conducted to evaluate its contribution to CRC progression. BALB/c nude mice were subcutaneously injected with HCT116 cells with either upregulated or downregulated METTL3 expression, thereby establishing CRC xenograft models (Fig. 4B). After 24 days, the mice were sacrificed and the tumor tissues were excised, weighed and imaged (Fig. 4C). The tumors from the METTL3 overexpression cells grew more rapidly and the tumor weights were heavier compared with the control cells, whereas knockdown of METTL3 significantly repressed tumor growth compared with the control cells (Fig. 4D). The tumors derived from cells with METTL3 overexpression exhibited significantly elevated METTL3 and MMP9 mRNA levels compared with the control group. Conversely, tumors from the METTL3 knockdown cells showed a significant reduction in METTL3 and MMP9 mRNA levels relative to the control group (Fig. 4E). The IHC results showed that the shMETTL3 HCT116 xenograft exhibited lower expression levels of METTL3 and MMP9 than the control xenografts, while METTL3-overexpression HCT116 xenograft exhibited higher expression levels of METTL3 and MMP9 (Fig. 4F). In summary, the findings indicated that the m^{6}A modification facilitated by METTL3 promoted CRC development by upregulating MMP9 expression *in vivo*.

Discussion

RNA modification has been steadily revealed for decades and at least 170 different post-transcriptional RNA modifications have been identified, among which the most common RNA modifications are m^{6}A, m^{1}A, m^{5}C, hm^{5}C, Ψ and 5-methoxyuracil (30,31). In eukaryotic cells, m^{6}A methylation is recognized as the most prevalent reversible modification occurring post-transcriptionally in RNA, constituting ~50% of total methylated ribonucleotides and 0.1-0.5% of all adenosine residues in the entire cellular RNA population (32). The results of the present study demonstrated that the m6A levels of CRC cell lines (HIEC-6 and NCM-460) account for >0.5%, while colorectal normal cell lines (LS174T, HCT-116 and SW480)

account for 0.2%, consistent with this finding. What's more, the global mRNA m^{6}A levels were highly elevated in CRC cell lines compared with colorectal normal cell lines, indicating a relationship between m^{6}A modification and CRC progression. Numerous studies have demonstrated that METTL3 is aberrantly expressed in a number of tumor types and is closely associated with the development of tumors (33-35). In the present study, it was found that METTL3 was significantly upregulated in CRC, in agreement with previous studies. More notably, in the xenograft model analysis, overexpression of METTL3 effectively promoted subcutaneous tumor growth in nude mice, and vice versa. This corroborative evidence further confirmed that dysregulation of METTL3 may be involved in CRC progress. The findings also imply that METTL3 plays a pivotal role in promoting CRC malignant progression. This suggests that developing modulators targeting m^{6}A and METTL3 could offer promising new therapeutic strategies for combating CRC.

M^{6}A modification is, in general, functionally interpreted by m^{6}A reader proteins (36). The reader proteins can recognize and bind m^{6}A modifications, allowing them to facilitate the gene regulatory functions of m^{6}A (33). Previous research has shown that IGF2BP1-3 and YTH N6-methyladenosine RNA binding protein F1 function as m^{6}A readers, recognizing m^{6}A modifications and thereby enhancing the stability of the corresponding mRNA (37). The results of the present study showed that METTL3 could stabilize MMP9 mRNA in a m^{6}A-dependent manner via Act-D analysis, indicating the interplay between the m^{6}A reader and the m^{6}A modification of MMP9 mRNA requires further investigation. To comprehend the biological significance of RNA m^{6}A modifications, it is essential to identify m^{6}A modification sites across the entire transcriptome. The mechanism by which the m^{6}A site on MMP9 mRNA affects the mRNA longevity via methylation by METTL3 needs to be further explored.

MMP9, a zinc-dependent proteolytic enzyme, possesses the capability to break down ECM components, playing a crucial role in various pathophysiological processes (38). Formerly described transcriptional control of MMP9 consists of histone modifications and microRNA (39,40). In the present study, it was firstly found that MMP9 mRNA could be methylated and that METTL3 could catalyze MMP9 mRNA m^{6}A methylation and further promote its expression through enhancing the m^{6}A-modified MMP9 mRNA stability, thus affecting the migration and proliferation of CRC *in vitro*. Furthermore, the critical involvement of METTL3 in CRC was verified experimentally using the subcutaneous transplantation model, which suggested a possible therapeutic intervention for cancer progression by targeting the novel MMP9 epigenetic modification.

However, the present study has certain limitations. The number of animals used in the study was limited to 5 per group. A small sample size can restrict the statistical power of the study, making it difficult to detect significant effects or differences. Furthermore, the present study did not incorporate clinical specimens, which limits the ability to empirically validate the findings. Without direct evidence from patient samples, the applicability of the results to real-world clinical scenarios remains uncertain. Additionally, only HCT-116 cell lines were utilized in the animal experiments. The deficiency of additional cell lines for validation restricts the ability to confirm the mechanisms proposed in the present study. Without corroborating evidence from other relevant models, the findings regarding role of METTL3 in promoting tumorigenesis via MMP9 remains less robust. Future investigations should prioritize the inclusion of a broader range of cell lines and models to enhance the robustness and applicability of the results.

In summary, the results of the present study indicated METTL3 was frequently upregulated in CRC and closely related to the clinicopathological features. Moreover, upregulation of METTL3 promoted CRC cell proliferation and tumorigenesis by enhancing MMP9 expression and it was discovered that the m^{6}A modification of MMP9 may be involved in the molecular mechanisms of these observed functional behaviors in CRC. The results of the present study therefore indicated that concurrently targeting METTL3 and MMP9 could offer novel therapeutic avenues for the treatment of CRC.

Acknowledgements

Not applicable.

Funding

This study was financially supported by Jiaxing City and Provinces to Build Medical Key Disciplines-Oncology (grant no. 2023-SSGJ-001) and National Oncology Clinical Key Specialty (grant no. 2023-GJZK-001).

Availability of data and materials

The data generated in the present study may be requested from the corresponding author.

Authors' contributions

JC performed most of the experiments and data analysis. JC, HW, TZ and JW assisted in the *in vivo* or *in vitro* experiments. JC and ZC wrote the original manuscript draft. JW contributed to experimental guidance. JC, JW and ZC designed the project and revised and edited the manuscript. All authors have read and approved the final version of the manuscript. JC and ZC confirm the authenticity of all the raw data.

Ethics approval and consent to participate

Animal experiments were approved by the Animal Experimental Ethics Committee of the First Affiliated Hospital of Jiaxing University (Jiaxing, China; approval no. JXYY2024-021).

Patient consent for publication

Not applicable.

Competing interests

The authors declare that they have no competing interests.

References

1. Siegel RL, Wagle NS, Cercek A, Smith RA and Jemal A: Colorectal cancer statistics, 2023. CA Cancer J Clin 73: 233-254, 2023.
2. Wolf D, Salcher S and Pircher A: The multivisceral landscape of colorectal cancer metastasis: Implications for targeted therapies. J Clin Invest 134: e178331, 2024.
3. Association NHCOTPROCSOOCM: National Health Commission guidelines for diagnosis and treatment of colorectal cancer 2023 in China (English version). Chin J Cancer Res 35: 197-232, 2023.
4. Bien J and Lin A: A review of the diagnosis and treatment of metastatic colorectal cancer. Jama-J Am Med Assoc 325: 2404-2405, 2021.
5. Miranda E, Bianchi P, Destro A, Morenghi E, Malesci A, Santoro A, Laghi L and Roncalli M: Genetic and epigenetic alterations in primary colorectal cancers and related lymph node and liver metastases. Cancer 119: 266-276, 2013.
6. Clemens AW, Lin S, Jain S, Su YH and Song W: Detection of colorectal cancer-associated genetic and epigenetic alterations in urine of patients with CRC. Cancer Res 75: abs. 1561, 2015. https://doi.org/10.1158/1538-7445.AM2015-1561.
7. Nosho K, Kawasaki T, Ohnishi M, Suemoto Y, Kirkner GJ, Zepf D, Yan L, Longtine JA, Fuchs CS and Ogino S: mutation in colorectal cancer: Relationship with genetic and epigenetic alterations. Neoplasia 10: 534-541, 2008.
8. Jiang XL, Liu BY, Nie Z, Duan L, Xiong Q, Jin Z, Yang C and Chen Y: The role of m6A modification in the biological functions and diseases. Signal Transduct Tar 6: 74, 2021.
9. Roundtree IA, Luo GZ, Zhang Z, Wang X, Zhou T, Cui Y, Sha J, Huang X, Guerrero L, Xie P, *et al*: YTHDC1 mediates nuclear export of N^6 - methyladenosine methylated mRNAs. Elife 6: e31311, 2017.
10. Zhu ZM, Huo FC, Zhang J, Shan HJ and Pei DS: Crosstalk between m6A modification and alternative splicing during cancer progression. Clin Transl Med 13: e1460, 2023.
11. Fang Z, Mei WT, Qu C, Lu J, Shang L, Cao F and Li F: Role of m6A writers, erasers and readers in cancer. Exp Hematol Oncol 11: 45, 2022.
12. Liu J, Yue Y, Han D, Wang X, Fu Y, Zhang L, Jia G, Yu M, Lu Z, Deng X, *et al*: A METTL3-METTL14 complex mediates mammalian nuclear RNA N6-adenosine methylation. Nat Chem Biol 10: 93-95, 2014.
13. Ping XL, Sun BF, Wang L, Xiao W, Yang X, Wang WJ, Adhikari S, Shi Y, Lv Y, Chen YS, *et al*: Mammalian WTAP is a regulatory subunit of the RNA N6-methyladenosine methyltransferase. Cell Res 24: 177-189, 2014.
14. Yue Y, Liu J, Cui X, Cao J, Luo G, Zhang Z, Cheng T, Gao M, Shu X, Ma H, *et al*: VIRMA mediates preferential m^6A mRNA methylation in 3'UTR and near stop codon and associates with alternative polyadenylation. Cell Discov 4: 10, 2018.
15. Patil DP, Chen CK, Pickering BF, Chow A, Jackson C, Guttman M and Jaffrey SR: m(6)A RNA methylation promotes XIST-mediated transcriptional repression. Nature 537: 369-373, 2016.
16. Zheng G, Dahl JA, Niu Y, Fedorcsak P, Huang CM, Li CJ, Vågbø CB, Shi Y, Wang WL, Song SH, *et al*: ALKBH5 Is a Mammalian RNA Demethylase that Impacts RNA Metabolism and Mouse Fertility. Mol Cell 49: 18-29, 2013.
17. Jia G, Fu Y, Zhao X, Dai Q, Zheng G, Yang Y, Yi C, Lindahl T, Pan T, Yang YG and He C: 6-Methyladenosine in nuclear RNA is a major substrate of the obesity-associated FTO. Nat Chem Biol 7: 885-887, 2011.
18. Li T, Hu PS, Zuo Z, Lin JF, Li X, Wu QN, Chen ZH, Zeng ZL, Wang F, Zheng J, *et al*: METTL3 facilitates tumor progression via an mA-IGF2BP2-dependent mechanism in colorectal carcinoma. Mol Cancer 18: 112, 2019.
19. Sun Y, Gong W and Zhang S: METTL3 promotes colorectal cancer progression through activating JAK1/STAT3 signaling pathway. Cell Death Dis 14: 765, 2023.
20. Xiang S, Liang XL, Yin S, Liu J and Xiang Z: N6-methyladenosine methyltransferase METTL3 promotes colorectal cancer cell proliferation through enhancing MYC expression. Am J Transl Res 12: 1789-1806, 2020.
21. Zhou D, Tang W, Xu Y, Xu Y, Xu B, Fu S, Wang Y, Chen F, Chen Y, Han Y and Wang G: METTL3/YTHDF2 m6A axis accelerates colorectal carcinogenesis through epigenetically suppressing YPEL5. Mol Oncol 15: 2172-2184, 2021.
22. Zhu W, Si Y, Xu J, Lin Y, Wang JZ, Cao M, Sun S, Ding Q, Zhu L and Wei JF: Methyltransferase like 3 promotes colorectal cancer proliferation by stabilizing CCNE1 mRNA in an m6A-dependent manner. J Cell Mol Med 24: 3521-3533, 2020.
23. Mondal S, Adhikari N, Banerjee S, Amin SA and Jha T: Matrix metalloproteinase-9 (MMP-9) and its inhibitors in cancer: A minireview. Eur J Med Chem 194: 112260, 2020.
24. Marshall DC, Lyman SK, McCauley S, Kovalenko M, Spangler R, Liu C, Lee M, O'Sullivan C, Barry-Hamilton V, Ghermazien H, *et al*: Selective Allosteric Inhibition of MMP9 is efficacious in preclinical models of ulcerative colitis and colorectal cancer. PLoS One 10: e0127063, 2015.
25. Choi SH, Lee HJ, Jin YB, Jang J, Kang GY, Lee M, Kim CH, Kim J, Yoon SS, Lee YS and Lee YJ: MMP9 Processing of HSPB1 Regulates Tumor Progression. PLoS One 9: e85509, 2014.
26. Lee MA, Park JH, Rhyu SY, Oh ST, Kang WK and Kim HN: Wnt3a expression is associated with MMP-9 expression in primary tumor and metastatic site in recurrent or stage IV colorectal cancer. BMC Cancer 14: 125, 2014.
27. Bauer L, Takacs A, Slotta-Huspenina J, Langer R, Becker K, Novotny A, Ott K, Walch A, Hapfelmeier A and Keller G: Clinical significance of NOTCH1 and NOTCH2 expression in gastric carcinomas: An immunohistochemical study. Front Oncol 5: 94, 2015.
28. Livak KJ and Schmittgen TD: Analysis of relative gene expression data using real-time quantitative PCR and the 2(-Delta Delta C(T)) Method. Methods 25: 402-408, 2001.
29. Boonsongserm P, Angsuwatcharakon P, Puttipanyalears C, Aporntewan C, Kongruttanachok N, Aksornkitti V, Kitkumthorn N and Mutirangura A: Tumor-induced DNA methylation in the white blood cells of patients with colorectal cancer. Oncol Lett 18: 3039-3048, 2019.
30. Barbieri I and Kouzarides T: Role of RNA modifications in cancer. Nat Rev Cancer 20: 303-322, 2020.
31. Chen Z, Zhao P, Li FY, Wang Y, Smith AI, Webb GI, Akutsu T, Baggag A, Bensmail H and Song J: Comprehensive review and assessment of computational methods for predicting RNA post-transcriptional modification sites from RNA sequences. Brief Bioinform 21: 1676-1696, 2020.
32. Roundtree IA, Evans ME, Pan T and He C: Dynamic RNA Modifications in gene expression regulation. Cell 169: 1187-1200, 2017.
33. Zeng C, Huang W, Li Y and Weng H: Roles of METTL3 in cancer: Mechanisms and therapeutic targeting. J Hematol Oncol 13: 117, 2020.
34. Chen H, Pan Y, Zhou Q, Liang C, Wong CC, Zhou Y, Huang D, Liu W, Zhai J, Gou H, *et al*: METTL3 Inhibits Antitumor Immunity by Targeting m^6A-BHLHE41-CXCL1/CXCR2 Axis to promote colorectal cancer. Gastroenterology 163: 891-907, 2022.
35. Wei X, Huo Y, Pi J, Gao Y, Rao S, He M, Wei Q, Song P, Chen Y, Lu D, *et al*: METTL3 preferentially enhances non-mA translation of epigenetic factors and promotes tumourigenesis. Nat Cell Biol 24: 1278-1290, 2022.
36. Zaccara S, Ries RJ and Jaffrey SR: Reading, writing and erasing mRNA methylation. Nat Rev Mol Cell Biol 20: 608-624, 2019.
37. Huang H, Weng H, Sun W, Qin X, Shi H, Wu H, Zhao BS, Mesquita A, Liu C, Yuan CL, *et al*: Recognition of RNA N^6-methyladenosine by IGF2BP proteins enhances mRNA stability and translation. Nat Cell Biol 20: 285-295, 2018.
38. Mizuno R, Kawada K, Itatani Y, Ogawa R, Kiyasu Y and Sakai Y: The role of tumor-associated neutrophils in colorectal cancer. Int J Mol Sci 20: 529, 2019.
39. Song Z, Yang L, Hu W, Yi J, Feng F and Zhu L: Effects of histone H4 hyperacetylation on inhibiting MMP2 and MMP9 in human amniotic epithelial cells and in premature rupture of fetal membranes. Exp Ther Med 21: 515, 2021.
40. Pirooz HJ, Jafari N, Rastegari M, Fathi-Roudsari M, Tasharrofi N, Shokri G, Tamadon M, Sazegar H and Kouhkan F: Functional SNP in microRNA-491-5p binding site of MMP9 3-UTR affects cancer susceptibility. J Cell Biochem 119: 5126-5134, 2018.